5-1-1990

Slippery Near-Surface Layer of the Ocean Arising Due to Daytime Solar Heating

Vladimir N. Kudryavtsev
Marine Hydrophysical Institute - Sevastopol, USSR

Alexander Soloviev
USSR Academy of Sciences - Moscow, soloviev@nova.edu

Slippery Near-Surface Layer of the Ocean Arising Due to Daytime Solar Heating

VLADIMIR N. KUDRYAVTSEV

Marine Hydrophysical Institute, Sevastopol, USSR

ALEXANDER V. SOLOVIEV

P. P. Shirshov Institute of Oceanology, USSR Academy of Sciences, Moscow, USSR

(Manuscript received 6 June 1989, in final form 25 September 1989)

ABSTRACT

Measurements made in the Equatorial Atlantic during the 35th cruise of the R/V *Akademic Vernadsky* using a free-rising profiler and drifters revealed a near-surface slippery layer of the ocean arising due to daytime solar heating. The solar heating warms and stabilizes the surface layer of the ocean. This suppresses turbulent exchange and limits the penetration depth of the wind-induced turbulent mixing. The heated near-surface layer is then slipping over the underlying water practically without friction. At daytime warming of 1°C the resistance coefficient in the upper 5-m ocean, $C_u = (U_*/\Delta U_s)^2$, became smaller by a factor of 25–30 as compared with the case of neutral stratification. The effect of slipping results in forming a daytime near-surface current. At low wind speed the velocity of this current was observed to achieve 19 cm s^{-1}. A simple one-dimensional integral model reproduces the main diurnal variation of the temperature and the current velocity in the near-surface layer of the ocean.

For daytime the experimental data suggest the existence of a self-regulating state of the diurnal thermocline, which predicts linear temperature and velocity profiles and an equilibrium value of the bulk Richardson number. This provides simple relations coupling the temperature and velocity differences and the thickness of thermocline. An estimation of the upper velocity limit of the daytime near-surface current is equal to 29 cm s^{-1}.

1. Introduction

The effect of decreasing turbulent friction due to the action of buoyancy in a stably stratified flow is well-known in the theory of turbulence. One can observe this effect in the atmosphere during dust storms (Barenblatt and Golitsin 1973), over glaciers and at night, if stable stratification occurs in the near-ground layer. This also applies to bottom turbidity currents (Turner 1973).

During daytime the absorption of solar radiation produces a positive buoyancy flux, which contributes to the stability of the upper ocean. In this case the depth of the wind-mixed layer may be scaled with the Oboukhov length,

$$L_* = U_*^3/(\alpha g Q_0/c_p\rho)$$

where U_* is the dynamic velocity in the surface of the ocean layer, Q_0 the resultant heat flux entering the ocean through its surface,[1] g the acceleration of gravity, α the coefficient of thermal expansion, c_p the specific heat capacity, and ρ the density of water. The depth scale of the Ekman boundary layer is given by $L_E = U_*/f$, where f is the Coriolis parameter. It is well known that the turbulent near-surface flow is dominated by the buoyancy force when $L_*/L_E = U_*^2 f(\alpha g Q_0/c_p\rho)^{-1} \ll 1$. Hence, the friction velocity U_* decreasing, the influence of the buoyancy force rises. A similar effect is observed when approaching the equator where the Coriolis parameter goes to zero.

Thus, the slippery effect of diurnal heating of the ocean layer should be more conspicuous in regions of low wind speed. Also, the wind velocity range (when the slippery effect is likely to be significant) becomes larger in the vicinity of the equator.

Woods (1968) has noted that turbulent friction decreases in high-temperature gradient sheets of the ocean. He has concluded that the water above a strong thermocline is capable of sliding over the underlying water with a minimum of friction (see Houghton

Corresponding author address: Dr. A. V. Soloviev, P. P. Shirshov Institute of Oceanology, USSR Academy of Sciences, Krasicova 23, Moscow 117851, USSR.

[1] The more accurate approach requires consideration of the effect of volume absorption of the radiation and corresponding modification of the L_*-scale (see section 4).

1969). To describe this effect, Houghton (1969) has used the term "slippery seas."

Houghton (1969) has observed the "slippery seas" in the coastal region at Acapulco. He has associated the occurrence of stable stratification in the near-surface ocean layer with the regional currents rather than with a daytime solar heating. Hence, Houghton (1969) has not connected the "slippery seas" with a diurnal jet.

Montgomery and Stroup (1962) have observed the equatorial region surface currents arising due to solar heating, but have obtained only fragmentary data. According to Bruce and Firing (1974) and Soloviev and Vershinsky (1982), at weak wind events the daytime heating is localized in a very thin near-surface layer of the ocean (the depth scale is about 1 m).

Recently, Woods and Strass (1986) and Price et al. (1986) have carried out fine studies concerning the response of wind-driven currents to solar heating. But their analysis did not include experimental data obtained under low-wind speed conditions when the daytime heating is localized in the 1-m upper ocean.

The goal of this paper is to study the effect of a slipping near-surface layer of the ocean arising due to daytime solar heating under conditions of low wind speed. For this purpose we used a tethered free-rising profiler developed by Soloviev et al. (1988), which measured small-scale turbulence and stratification in the near-surface layer of the ocean. A two-drifter system (Egorikhin et al. 1976) has permitted us to study the wind-driven currents.

2. Experimental procedure

a. Drifters

We measured the velocity difference in the near-surface layer of the ocean by means of two drifters tracing the ocean surface (Egorikhin et al. 1976). Figure 1a schematically shows the drifters' design. It consists of a surface float (1), a drogue (2) located just under the sea surface or at a 5-m depth, a weight (3), and a 2-mm steel cable (4). The drogue is made of two vertically mounted planes, each being 0.7×1 m^2. The drag area ratio of the drifters between the drogue and the surface float is about 50. The drogue of the first drifter was just under the sea surface (centered at 0.35 m depth), the drogue of the second one was centered at 5-m depth.

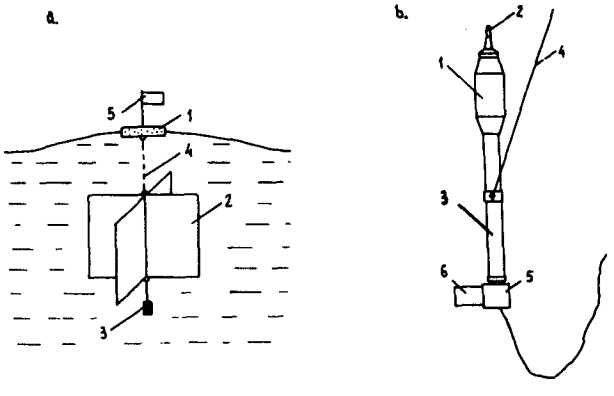

FIG. 1. Scheme of (a) the drifter and (b) the tethered free-rising profiler.

The drifters were simultaneously deployed from a boat about 0.5 to 1 km away from the vessel. Observational time interval (Δt_0) was 20 min. At the end of the time interval (prior to retrieval of the drifters) we determined the distance between them. For this, the boat equipped with an antenna reflector approached in turn the drifter surface floats, its position being monitored by the radar mounted on the drifting vessel. We determined the bearing and the distance of each drifter. This helped calculate the difference vector, $\Delta\vec{l}$, showing divergence of the drifters. Then, a simple formula $\Delta\vec{U}_s = \Delta\vec{l}/\Delta t_0$ gave the vector of current velocity difference, $\Delta\vec{U}_s$, between the drogue depths (0.35 and 5 m).

The time interval between observations of the first and the second drifter ($\Delta t_0'$) was about 1 min. During this time the vessel (from which the radar measurements were being made) was drifting in response to the wind thus producing a regular error of 1 to 2 cm s^{-1}. To eliminate it we have introduced a drift correction using the formula: $\Delta\vec{U}_s' = \vec{V}_d\Delta t_0'/\Delta t_0$, where $\vec{V}_d$ is the vector of wind-drift velocity of the vessel given by the relation: $\vec{V}_d = \beta\vec{V}_{20}$, where $\vec{V}_{20}$ is the wind speed vector at 20-m level above the ocean. For *Akademic Vernadsky* the value of the drift coefficient $\beta = 4.5 \times 10^{-2}$ was experimentally obtained by means of a current meter lowered from the drifting vessel at different wind speeds, V_{20}.

An error in determining ΔU_s using the technique described above is coupled with the accuracy of distance measurements by the radar, $\delta l_i = \pm 18$ m, which, with the observational time interval being 20 min, corresponded to $\delta(\Delta U_s) = \pm 1.5$ cm s^{-1}.

An increase of the observational time interval, Δt_0, decreases this error. But another error of the following origin would arise. The near-surface drifters can be captured by Langmuir circulation lines or other convergences coinciding with the wind direction and then carried along, trapped in the regions of convergence. According to Filatov et al. (1981), in these regions physical parameters of the near-surface layer differ from the outside flow and are not representative of either the flow outside the convergences or the average flow. An exact estimation of the error of this type presently is not possible because under conditions of low-wind speed and strong temperature gradients in the upper meters the Langmuir circulation is insufficiently studied.

In any case, during our measurements of the slippery near-surface layer we did not visually observe any cells or distinct convergences along the wind direction. Probably, the Langmuir circulation did not occur at low wind speed (2.5–4.5 m s^{-1}). Therefore, we considered the errors in the velocity measurements produced by Langmuir cells to be small. Occasionally we observed slick lines produced by internal waves on the ocean surface. But the lines did not coincide with the wind direction and according to our visual observations, did not capture the drifters.

b. *Free-rising profiler*

Small-scale turbulence in the near-surface layer of the ocean was measured from the drifting ship using a profiler developed by Soloviev et al. (1988). The unit is shown schematically in Fig. 1b; it is a tethered free-rising device with microstructure sensors of velocity and conductivity (2) mounted on its nose. The profiler body (3) is a 1-m long cylinder, 56 mm in diameter, containing electronics and mercury batteries. A flotation collar (1), 12 cm in diameter and 30 cm long, is mounted on the upper part of the profiler body.

The instrument is deployed from an 8-meter forward boom with the vessel broadside to the wind. Prior to profiling the instrument coupled with a ballast electromagnet (5) is set overboard on a tethered line (4). A fin (6) mounted on the body of the ballast electromagnet allows the instrument to move away from the ship's wake.

When the ballast weight is dropped, buoyancy becomes positive and the profiler rises the surface with a nominal speed of 2.2 m s^{-1} trailing the tethered line. Measurements are made during ascent. Influence of the ship's motion is reduced considerably, as the mechanical load is removed from the tethered line. The instrument is operational to wind speed $V_{20} \leqslant 7.5$–8 m s^{-1} and wave height $H_w \leqslant 1.5$–2 m.

The velocity sensor is of electromagnetic type. The sensing unit has a streamlined form with hemispherical nose 6 mm in radius. The electrodes of electromagnetic sensing unit simultaneously serve as a conductivity cell due to frequency separation in the electric circuits. The velocity sensor operates at a frequency range 2 to 500 Hz, the conductivity sensor on a carrier frequency of 600 kHz. Using a single sensing unit for measuring all of the parameters decreases noise level due to vortex shedding. This is important for microstructure measurements in the near-surface layer where surface wave disturbances may be significant. Spatial resolution of the sensors is about 1 cm.

Temperature profiles in the surface layer of the ocean were obtained on the basis of conductivity profiles neglecting salinity variations. According to Soloviev and Vershinsky (1982), conductivity profiles in the near-surface layer of the ocean nearly always repeat the corresponding temperature profiles with the exception of rainfall events. The vertical temperature profiles were used to define temperature difference between the drogue depths, the depth of the diurnal mixed layer, H, and the thickness of the diurnal thermocline, h. To improve statistical validity the profile measurements were repeated several times.

c. *Measurements*

During the 35th cruise the R/V *Akademic Vernadsky* carried out hydrology stations in the equatorial Atlantic according to the USSR national project RAZREZY. At a number of stations we studied the response of the thin near-surface layer of the ocean to daytime solar heating. Measurements were made in February–March 1987 in the area with coordinates 8°N and 1°S, 22° and 33°W.

A station normally takes 40 to 60 min. We carried out the measurements in the following manner. A boat deployed drifters about 0.5–1 km away from the vessel. Twenty minutes after deployment we measured the distance between the drifters and then calculated the velocity difference, ΔU_s, between the drogue depths (0.35 and 5 m). Temperature difference between the appropriate depths (0.35 and 5 m), ΔT_s, was measured from the boat using a standard reversing thermometer. At the same time, a free-rising profiler measured from the vessel the conductivity profiles and, in some cases, the turbulence velocity profiles. Meteorology service on board *Akademic Vernadsky* issued hourly weather observations of wind speed at 20-m level above the ocean (V_{20}), surface water temperature (T_w), air temperature (T_a), relative humidity (e), characteristics of clouds (N_Σ, N_L), surface waves, etc.

Friction velocity in the surface layer of the ocean (U_*) was calculated as

$$U_* = C_{20}^{1/2}(\rho_a/\rho)^{1/2}V_{20},$$

where C_{20} is the drag coefficient ($C_{20} = 1.3 \times 10^{-3}$), ρ_a and ρ are air and water densities. Sensible (Q_T) and latent (Q_L) heat turbulent fluxes were also calculated using appropriate bulk formulae. Incident (Q_Σ) and reflected (R_Σ) solar fluxes, and effective longwave radiation flux (Q_E) were measured directly.

During the measurements the sea surface state roughly resembled appropriate wind speed. On 1, 2 and 5 March we observed swell waves with lengths of 150–180 m and heights of about 1.5–2 m, 0.5–1 m and 1 m respectively. The relative angle between wind waves and swell was 30°, 140° and 10°, respectively.

Figures 2 and 3 represent the data obtained during our experiments. Figure 2 shows the vertical temperature profiles measured by the free-rising profiler. The profiles characterize a variety of situations that occur in the near-surface oceanic layer due to daytime solar heating. In most cases the temperature profiles dis-

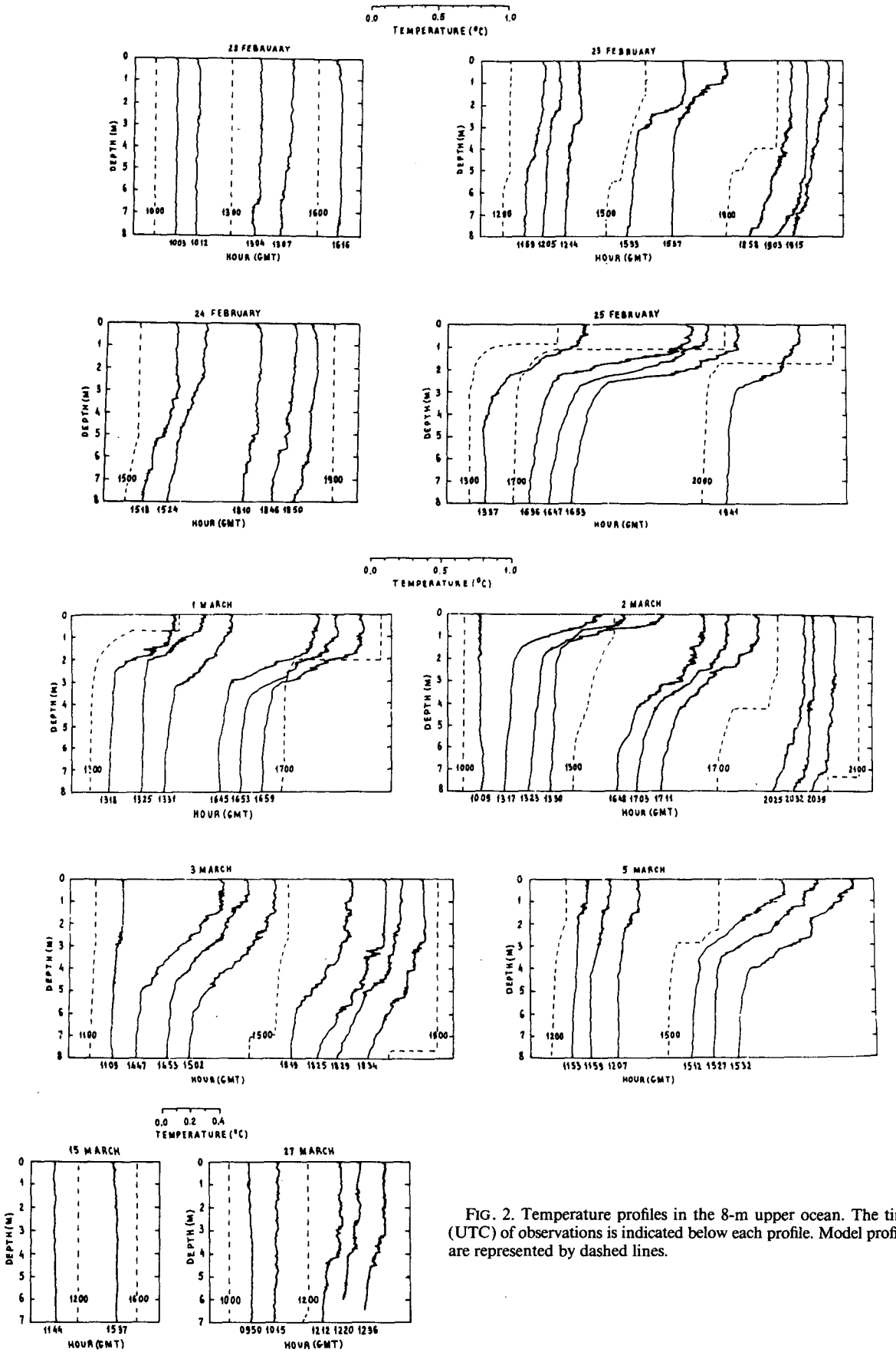

FIG. 2. Temperature profiles in the 8-m upper ocean. The time (UTC) of observations is indicated below each profile. Model profiles are represented by dashed lines.

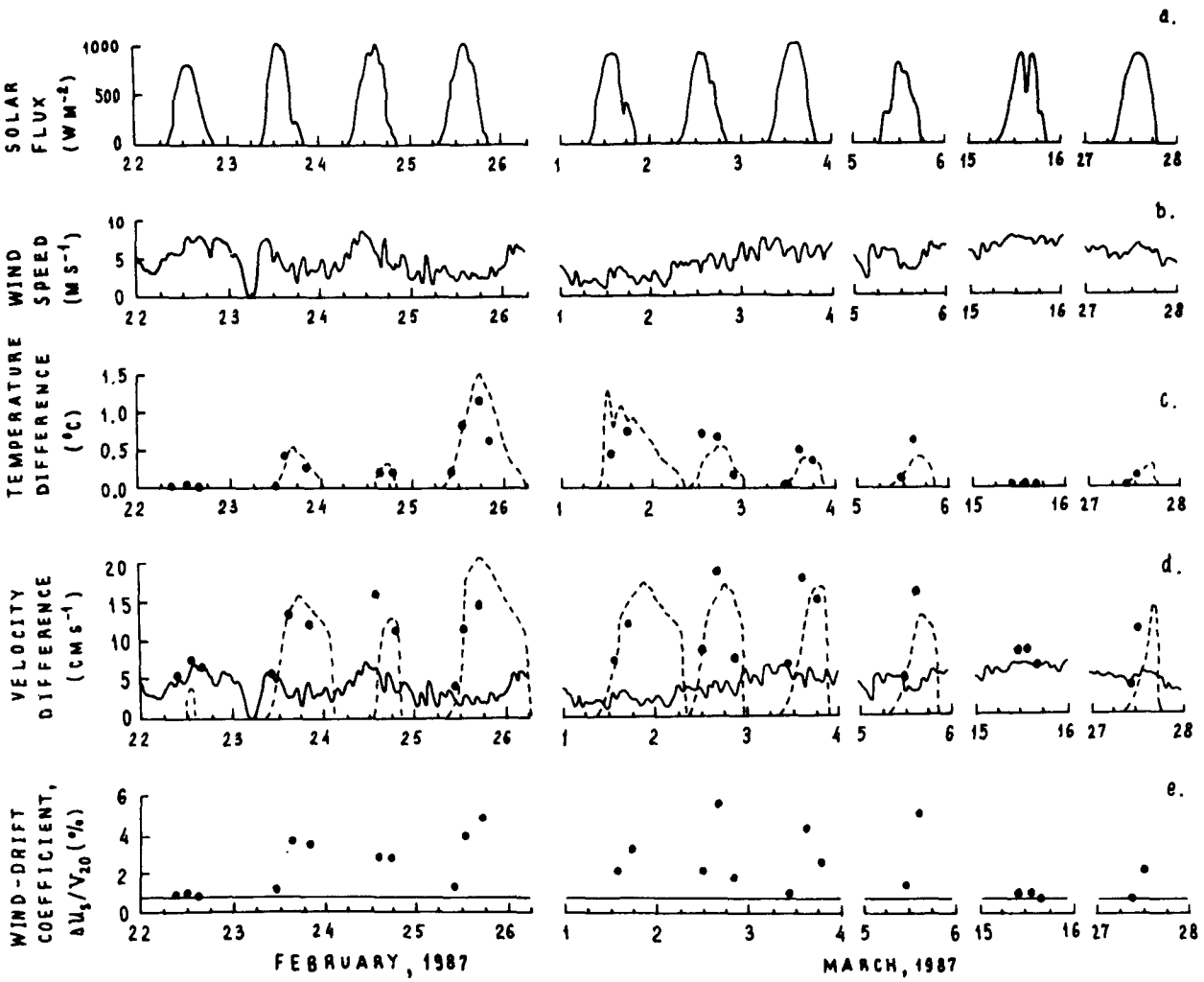

FIG. 3. Measurements in the Equatorial Atlantic and model-computed data encompassing the period from 22 February to 27 March, 1987. Time is UTC. (a) Solar radiation flux. (b) Wind speed at 20-m level above the ocean. (c) Temperature difference between the drogue depths (0.35 and 5 m) observed from a boat (points) and model-computed time series of the temperature difference between the surface and 10-m depth (dashed line). (d) Current velocity difference between the drodue depths (0.35 and 5 m) registered by the drifters (points) and the model-computed time series of the current velocity difference between the surface and 10-m depth (dashed line). Solid line corresponds to the current velocity difference calculated between 0.35 and 5 m depth for an unstratified constant stress layer using formula (1). (e) Coefficient of wind drift: measured (points). Solid line corresponds to formulae (1).

tinctly reveal the diurnal mixed layer and thermocline. Figure 3 shows evolution of the major meteorological parameters alongside with variability of the temperature and velocity differences in the surface layer, and the wind-drift coefficient evolution.

3. Experimental results

Figure 4 shows the effect of daytime heating on turbulence in the near-surface ocean layer at low wind speed. Three soundings made in the morning on 16 February demonstrate that solar heating noticeably restricts the depth of turbulence penetration. As the vertical profile σ_w (σ_w^2 is the dispersion of velocity pulsation) indicates, the turbulence occurs mainly within the upper 2.5-m layer coinciding with the layer of daytime heating.

This example (Fig. 4) relates to the initial stage of diurnal warming immediately after an abrupt drop of wind speed from 7.2 m s^{-1} at 1200 UTC to 3.3 m s^{-1} at 1400 UTC. Due to this, temperature differences still remain relatively small (only 0.1–0.2°C). Here the diurnal mixed layer and diurnal thermocline are not distinctly identified since the temperature profiles change in time and have inversions. Such a situation is characteristic of the initial stage of diurnal warming. From this point of view, a near-surface inversion in the 1403 and 1408 temperature profiles seems to be accounted for by occasional lateral advection rather than by heat loss from ocean surface. An averaged

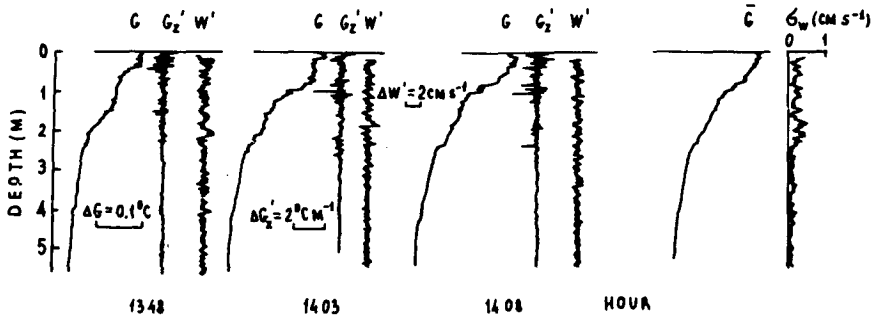

FIG. 4. A series of sounding made by the free-rising profiler. Here G is vertical temperature profiles, G'_z profiles of vertical temperature gradient, W' profiles of turbulent velocity pulsations, $\bar{G}$ a mean temperature profile, σ_w a profile of standard deviations of velocity turbulent pulsations ($\bar{G}$ and σ_w are averages of the three soundings). The time (UTC) of measurement for each sounding is indicated below.

temperature profile does not, indeed, reveal such an inversion.

Due to turbulence supression, the daytime heating should be accompanied by a decrease of the turbulence friction in the near-surface layer. Figure 5 shows the drag coefficient, $C_u = (U_*/\Delta U_s)^2$, dependence on the temperature difference, ΔT_s. Here ΔU_s is the velocity difference measured by drifters (between the drogue depths of 0.35 and 5 m); ΔT_s is the temperature difference between the levels at which the drogues were located. These data are indicative of a regular decrease of the drag coefficient in the near-surface layer when daytime heating increases. At the temperature difference $\Delta T_s \approx 1$°C the drag coefficient C_u became smaller by a factor of 25 to 30 as compared with the case of neutral stratification. During intensive daytime solar heating the thin near-surface layer is hence slipping practically without friction over underlying water.

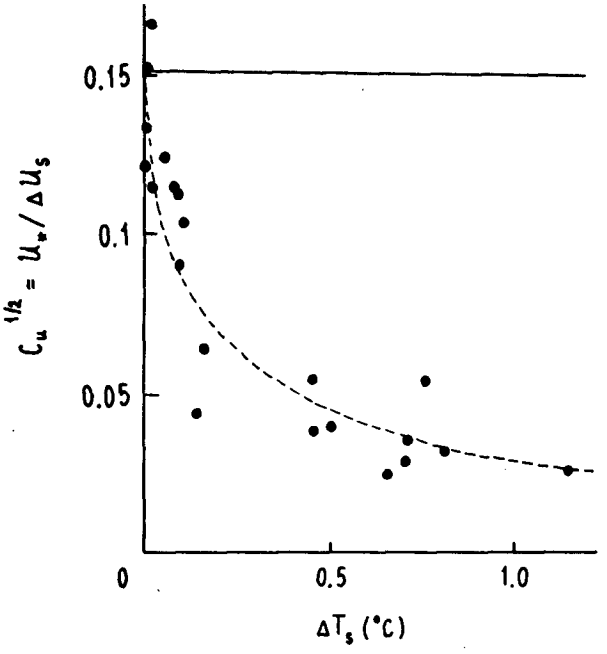

FIG. 5. Dependence of the drag coefficient, $C_u = (U_*/\Delta U_s)^2$, on the temperature difference, ΔT_s, in the morning and at noon time. Horizontal line corresponds to drag low in an unstratified layer with constant stress calculated from (1).

The slippery effect results in forcing a wind-driven current in the layer of daytime solar heating. Figure 3d shows experimental data (points) describing diurnal evolution of this daytime near-surface current. The current velocity difference, ΔU_s, is plotted together with solar radiation (a) and windspeed (b) time series, temperature difference (c) and appropriate wind-drift coefficient values (e). Vector ΔU_s had already been wind-oriented. The solid lines in diagram (d) and (e) correspond to the current velocity difference, ΔU_l, calculated between 0.35 and 5 m depths for an unstratified constant stress layer (logarithmic boundary layer),

$$\Delta U_l = V_{20}(C_{20}\rho_a/\rho)^{1/2}\kappa^{-1}\ln(5.0/0.35) \approx 0.85 \times 10^{-2}V_{20}. \quad (1)$$

The current velocity differences, ΔU_s, measured at wind speed $V_{20} \geq 7$ m s^{-1} (on 22 February and 15 March), when thermal stratification was negligible, were close to constant stress layer prediction (1). Whereas at wind speed $V_{20} \leq 5$ m s^{-1} the velocity difference, ΔU_s, distinctly increased during daytime as soon as the solar heating had thermally stratified the near-surface ocean layer. The velocity difference, ΔU_s, achieved maximum value in the afternoon of 2 March ($\Delta U_s \approx 19$ cm s^{-1}, $V_{20} = 4.4$ m s^{-1}). This value was to be larger by a factor of 5 than those correspondent to the constant stress layer prediction (1). Figure 3e demonstrates experimentally documented values of the wind-drift coefficient, $\Delta U_s/V_{20}$ (points). According to Fig. 3e the wind drift coefficient should be considered constant only at neutral stratification in the near-surface layer of the ocean. At large daytime heating the wind-drift coefficient was observed to increase by a factor of 5.

4. Physics

Slippery surface layers observed during daytime heating may be described in terms of the theory of turbulence in a stratified fluid. Tangential wind stress generates a near-surface current, which is heated from above by the sun. In such a current the turbulence mixing is known to form a near-surface mixed layer of depth H, which is proportional to the Oboukhov scale L_* (Turner 1973). Just below the mixed layer the buoyancy forces suppress turbulent mixing (see Fig. 4) thereby reducing the turbulent friction. Thus, the water constituting the mixed layer starts slipping as a whole over the water below.

In studying the near-surface layer of the ocean, possible wave effects should be analyzed. The nature of turbulence below the sea surface is now under investigation (Kitaigorodskii et al. 1983; Thorpe 1985; Cheung and Street 1988; Soloviev et al. 1988). Breaking surface waves may be an important source of turbulence at large wind speeds. But at low wind speeds the near-surface layer may exhibit some of the properties of a constant stress layer (Dillon et al. 1981). Small-scale turbulence measurements in the surface layer of the ocean carried out by Soloviev et al. (1988) suggested the departure of the dissipation rate from the constant stress layer prediction at low wind speeds as not being large enough. Cheung and Street (1988) determined in a laboratory facility that the waves affect mean flows, even though the profiles remain essentially logarithmic. In the wind-wave case they obtained the turbulent quantities to behave similarly to those in flows over flat plates.

The slippery near-surface layer arising from daytime solar heating has been most pronounced at low wind speeds. For this reason, as a first approximation, we did not consider wind wave influences here. Moreover, for the integral model, which will be used further, this question is of little importance because the term responsible for wave generation of turbulence can be included in the budget equation of turbulence energy in such a way that it will alter only the meaning of the constant m, which is finally being determined empirically (Niiler and Kraus 1977).

The daytime near-surface current can in turn affect the frequency spectra of the wind waves due to Doppler effect. But this question is beyond the subject of this paper.

a. One-dimensional integral model

We have simulated the slippery near-surface layer of the ocean, observed in the Equatorial Atlantic during the 35th cruise of the R/V *Akademic Vernadsky,* using a simple one-dimensional model similar to that of Niiler and Kraus (1977).

It is assumed that the model relative temperature, T, and current velocity, U, in the upper H-thick mixed layer are constant; below the latter the temperature and current velocity are decreasing smoothly or with discontinuities, approaching zero value that corresponds to seasonal mixed layer temperature and velocity.

1) EQUATIONS

For solar downward irradiance we have used a three-exponential dependence (Soloviev 1982),

$$S(z) = S_0 \sum_{i=1}^{3} A_i \exp(-\beta_i z),$$

where $S_0 = (c_p\rho)^{-1}(Q_\Sigma - R_\Sigma)$, Q_Σ is the incident solar energy flux and R_Σ is the flux reflected from the sea surface, $A_1 = 0.28$, $\beta_1 = 71.5\ \mathrm{m}^{-1}$, $A_2 = 0.27$, $\beta_2 = 2.8\ \mathrm{m}^{-1}$, $A_3 = 0.45$, $\beta_3 = 0.07\ \mathrm{m}^{-1}$, z is the depth.

After integrating within the mixed layer from $z = 0$ to $z = H$ the one-dimensional budget equations for heat, momentum and kinetic energy have the usual form (see Niiler and Kraus 1977),

$$H\partial_t T = \Delta S + q_0 - W_e\delta T, \tag{2}$$

$$H\partial_t U = U_*^2 - W_e\delta U, \tag{3}$$

$$(\alpha g H\delta T - c|\delta U|^2)W_e - 2mU_*^3 + \alpha g H[q_0 + (2/H) \times \int_0^H (\Delta S(z) - \Delta S(H)]dz) = 0, \tag{4}$$

where $\Delta S = S_0 - S(z)$, $q_0 = (Q_L + Q_T + Q_E)(C_p\rho)^{-1}$, ($Q_L$, Q_T and Q_E are the surface air–sea heat fluxes); W_e is the velocity of turbulent entertainment ($W_e = \partial_t H$ at $\partial_t H > 0$ and $W_e \equiv 0$ at $\partial_t H \leqslant 0$), δT and δU are the temperature and current velocity decrease at the lower boundary of the mixed layer, m and c are empirical nondimensional constants. Numerical value of the m-constant typically affects calculations of the mixed-layer depth in the morning and afternoon, whereas the c-constant controls the rate of mixed-layer deepening in the evening-time. In Eq. (3) the Coriolis force was ignored, because we considered an equatorial region. Also, in Eq. (4) the time derivative of the turbulent kinetic energy was neglected.

We have assumed that the region underlying the mixed layer ($z > H$) had no turbulence. Therefore, neglecting molecular viscosity we shall describe the temperature and current velocity evolution at $z < H$ as

$$\partial_t T = -\partial_z S, \tag{5}$$

$$\partial_t U = 0. \tag{6}$$

Equations (5), (6) were decided on the time interval $t_u < t < t_d$, i.e., between two sequential intersections of the fixed depth, z, by the lower boundary of the mixed layer. Relations, $H(tu) = z$ at $\partial_t H < 0$ and $H(t_d) = z$ at $\partial_t H > 0$, define the time interval (t_u, t_d) between two sequential intersections, at first, upwards ($t = t_u$),

and then, downwards ($t = t_d$), $T(t_u)$ and $U(t_u)$ being initial conditions for Eqs. (5), (6).

2) Preliminary model experiment

To see the qualitative behavior of the model we have carried out a simple experiment for which we set down the following conditions:

$$U_* = \text{const}_1, \quad q_0 = \text{const}_2 < 0, \quad c = 0,$$

$$S(t) = \begin{cases} S_0, & \text{at} \quad 0 < t \leqslant t_0 \\ 0, & \text{at} \quad t > t_0. \end{cases} \tag{7}$$

(In the preliminary model experiment volume absorbtion of solar radiation is not considered).

The model has given the relations:

$$H = 2m(\alpha g)^{-1}U_*^3(S_0 + q_0)^{-1}, \tag{8}$$

$$\Delta T = (2m)^{-1}\alpha g(S_0 + q_0)^2 U_*^{-3} t, \tag{9}$$

$$\Delta U = (2m)^{-1}\alpha g(S_0 + q_0)U_*^{-1} t, \tag{10}$$

at $0 < t \leqslant t_0$

$$H/H_0 = (1 + q_0 S_0^{-1})(1 + q_0 S_0^{-1} t t_0^{-1})^{-1} t t_0^{-1}, \tag{11}$$

$$\Delta T/\Delta T_0 = (1 + q_0 S_0^{-1} t t_0^{-1})^2 (1 + q_0 S_0^{-1})^{-2} t t_0^{-1}, \tag{12}$$

$$\Delta U/\Delta U_0 = (1 + q_0 S_0^{-1} t t_0^{-1})(1 + q_0 S_0^{-1}), \tag{13}$$

at $t > t_0$, where $\Delta T = T - T(0)$, $\Delta U = U - U(0)$, $H_0 = H(t_0)$, $\Delta U_0 = \Delta U(t_0)$, $\Delta T_0 = \Delta T(t_0)$.

Figure 6 shows the dependences (8)–(13) in nondimensional form. This simple model roughly describes evolution of the diurnal cycle of temperature and current velocity during daytime ($0 < t \leqslant t_0$) and nighttime ($t > t_0$). According to (8)–(10) during daytime the temperature and current velocity grow linearly with time, the mixed layer depth being constant. The thermal and current velocity responses are proportional to U_*^{-3} and U_*^{-1}, respectively. It is surprising that not only the diurnal cycle amplitude of the temperature, but also that of the current velocity tends to increase when the wind speed decreases. In a certain range of wind speeds this is qualitatively consistent with our observations (see Fig. 3).

At nighttime ($t > t_0$) the mixed layer deepens and temperature and current velocity are decreasing (Fig. 6). A feature of the nighttime evolution is that the temperature time dependence is concave while the velocity time dependence is linear.

3) Model results and comparison with experimental data

Model (2)–(6) has been computed at $m = 2$, $c = 0.1$ and $C_{20} = 1.3 \times 10^{-3}$. In Fig. 2 model temperature profiles (dashed curves) are compared with those obtained by the free-rising profiler.

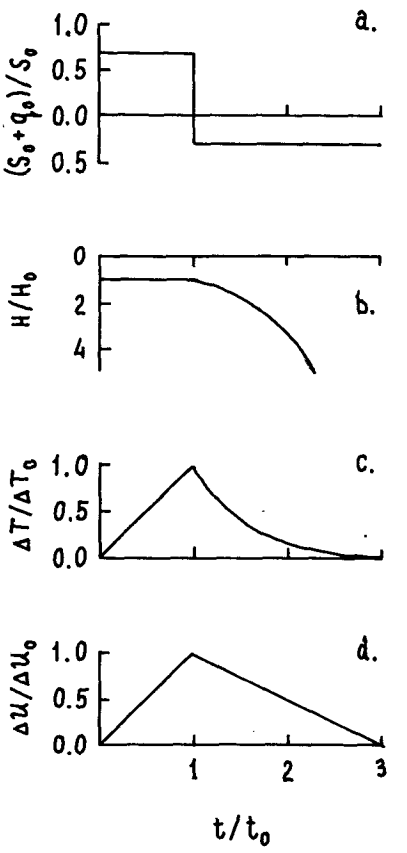

FIG. 6. Model experiment run. (a) Solar radiation model. Evolution of (b) mixed layer depth, (c) temperature and (d) current velocity are plotted in nondimentional coordinates for $q_0/(S_0 + q_0) = -0.3$.

In general, the model results correlate with the experimental profiles. The largest profile discrepancies are associated with temperature discontinuities at the bottom of the mixed layer, following from the nature of integral model.

A significant discrepancy between the model-simulated and experimental bulk temperature difference in the near-surface layer of the ocean has been observed about 1300 UTC 2 March (Fig. 2). This disagreement is assumed to result primarily from inaccuracy in determining momentum and heat fluxes at the ocean surface on the basis of the ship's meteorological information.

The model-simulated temperature and current velocity profiles were sampled to produce time series of temperature and velocity difference between the depth of 0.35 and 10 m for comparison with drifters data. The choice of 10 m rather than 5 m lower reference depth is more convenient since the model-simulated 0.35–10 m temperature and velocity differences are more stable with respect to small displacements of the bottom of the mixed layer. Dashed curves in Fig. 3 show the model-computed time series for the temperature (c) and velocity (d) difference.

On 22 February and 15 March, on days with wind speeds $V_{20} \geq 7$ m s^{-1}, both the model-simulated and experimentally obtained temperature differences in the near-surface layer of the ocean were negligible (Figs. 2, 3c). The experimental velocity differences were also respectively small and well described by logarithmic boundary layer prediction (1) (Fig. 3d). Hence, there was no appreciable slipping effect in the near-surface layer of the ocean on 22 February and 15 March.

On other days, with daytime wind speeds $V_{20} < 7$ m s^{-1}, amplitudes of diurnal variation of the model-simulated temperature difference were substantially increasing, so were the experimentally obtained temperature differences (Figs. 2, 3c). The appropriate experimental velocity differences (points on Fig. 3d) in daytime noticeably exceeded the logarithmic boundary layer prediction due to the slipping effect. They were generally in agreement with the integral model prediction (dashed curve on Fig. 3c).

It follows that a simple integral model describes at least the main properties of the slippery near-surface layer of the ocean occurring at low wind speeds due to daytime solar heating. A more adequate theoretical description of this effect can be done by application of a model including both the mixed layer and thermocline physics in the best way. Increasing accuracy of momentum and heat fluxes determination is also essential.

b. Self-regulating state of the daytime thermocline

As the above-considered two-layer model implies, the mixed layer is slipping over the underlying water mass. Its temperature and velocity are growing in the forenoon according to the laws

$$\Delta T \sim \Delta t U_*^{-3}, \tag{14}$$

$$\Delta U \sim \Delta t U_*^{-1}, \tag{15}$$

where Δt is the time interval.

In a two-layer model the discontinuity of the profiles T and U is an idealization. In reality, as Landau and Lifshits (1986) claim, the discontinuity of the tangential velocity distribution in incompressible fluid is unstable. Therefore, at the lower boundary of the mixed layer a transitional layer of definite thickness h (here the diurnal thermocline) is formed.

The bulk Richardson number of the diurnal thermocline can be defined as follows

$$\mathrm{Ri} = \alpha g \Delta T h / \Delta U^2, \tag{16}$$

where ΔT and ΔU are the bulk temperature and velocity differences in the thermocline, h the thickness of the thermocline. In daytime, the diurnal thermocline should control its thickness (h) in accord with the actual temperature (ΔT) and velocity (ΔU) difference by the criterion of the Richardson number equality to its equilibrium value Ri_0,

$$\mathrm{Ri} = \mathrm{Ri}_0, \tag{17}$$

ΔU and ΔT being controlled by the momentum and heat exchange at the ocean–atmosphere interface. A similar situation occurs at the external boundary layer of turbidity currents (Turner 1973). For a diurnal jet the concept of a critical gradient Richardson number has been used by Price et al. (1986). According to similarity theory for stratified flows with a self-regulating boundary layer the local gradients of temperature ($\partial_z T$) and velocity ($\partial_z U$) may be expressed through the buoyancy ($\alpha g \Delta T$) and velocity (ΔU) differences across the diurnal thermocline:

$$\alpha g \partial_z T = K_2 (\alpha g \Delta T / \Delta U)^2, \quad \partial_z U = K_1 \alpha g \Delta T / \Delta U, \tag{18}$$

where K_1 and K_2 are nondimensional constants.

Relations (18) describe linear temperature and velocity profiles. This is accounted for by the relations (18) no longer containing z as a variable. The interpretation is that in a stable boundary layer the vertical size of a turbulent eddy is restricted, so that turbulence could not be affected by the presence of the surface. As a result, the boundary layer structure no longer explicitly depends on z (Nieuwstadt 1984).

Figure 7 shows mean temperature profiles averaged over two or three sequential "instantaneous" profiles from those depicted in Fig. 2. Pertinent information to Fig. 7 is given in Table 1. In Fig. 7 we used only the profiles obtained under conditions of large daytime heating and when the lower boundary of the diurnal thermocline does not exceed 5 meters, i.e., the maximum drogue depth of the drifters.

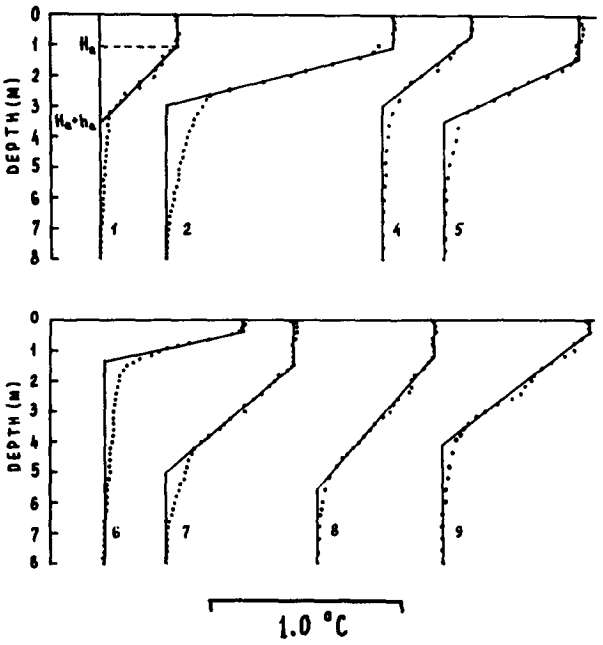

FIG. 7. Average temperature profiles. Numbering appropriates to Table 1.

TABLE 1. State of the diurnal thermocline at daytime under conditions of strong solar heating.

No.	Date (1987)	Time (UTC)	Time (LST)	Coordinates	V_{20} (m s^{-1})	Number of profiles	h_a (m)	ΔT_s (°C)	ΔU_s (cm s^{-1})	Ri
1	23 Feb	1533–1537	1351–1355	01°30′N, 22°01′W	3.9	2	2.5	0.45	13.1	0.19
2	25 Feb	1337	1159	02°29′N, 23°29′W	2.7	1	1.8	0.8	11.3	0.33
3	25 Feb	1636–1653	1451–1508	03°00′N, 23°30′W	2.9	3	1.8	1.15	14.3	0.30
4	1 Mar	1318–1331	1129–1142	06°30′N, 24°59′W	3.2	3	2.4	0.45	7.3	0.60
5	1 Mar	1645–1659	1456–1510	06°01′N, 25°00′W	3.3	3	2.0	0.7	11.8	0.30
6	2 Mar	1317–1330	1128–1141	03°03′N, 24°59′W	4.0	3	1.2	0.75	9.1	0.32
7	2 Mar	1648–1711	1510–1533	02°28′N, 24°59′W	4.4	3	3.8	0.7	19.0	0.22
8	3 Mar	1447–1502	1258–1313	00°28′N, 25°00′W	5.6	3	4.2	0.5	17.7	0.20
9	5 Mar	1512–1532	1316–1336	06°00′N, 26°30′W	3.0	3	3.7	0.65	15.6	0.29

According to Fig. 7 during daytime the profiles in the diurnal thermocline have linear intervals. An appreciable departure from linearity is observed only at the lower boundary of the diurnal thermocline. This departure is likely to be explained by the volume absorption of solar radiation below the diurnal thermocline. The remainder of "relict" diurnal thermoclines formed at the previous stages of daytime heating may also lead to the departures from linearity of the mean temperature profiles at the lower boundary of the thermocline.

Table 1 also gives experimentally obtained values of a bulk Richardson number, Ri. To evaluate the bulk Richardson number we used formula (16) and the assumptions, $\Delta T \approx \Delta T_s$, $\Delta U \approx \Delta U_s$, and $h \approx h_a$, where ΔT_s and ΔU_s are the temperature and current velocity differences between the drogue depths of the drifters, 0.35 and 5 m, h_a is the thickness of the diurnal thermocline obtained from a linear approximation of the mean profiles as shown in Fig. 7 (Table 1 lists the appropriate values of h_a).

The experimental data have proved (Table 1) that during daytime the bulk Richardson number, Ri is close to a critical value $\frac{1}{4}$($\langle \mathrm{Ri} \rangle = \mathrm{Ri}_0 = 0.3 \pm 0.1$) and the mean temperature profile in the daytime thermocline has nearly linear interval (Fig. 7). These data speak in favor of the self-regulating state of the diurnal thermocline (during daytime).

So, in the daytime thermocline temperature (and velocity) profiles may be approximated, as shown in Fig. 7, by a straight line. For model temperature and velocity profiles of this type heat ($c_p\rho\partial_t T = -\partial_z Q - \partial_z S$) and momentum ($\partial_t U = -\partial_z \tau/\rho$) exchange equations, integrated over depth and time, take a following simple form:

$$\Delta U(H + 0.5h) = \int_0^t (\tau_0/\rho)dt, \qquad (19)$$

$$\Delta T(H + 0.5h) = \int_0^t (Q_0/c_p\rho)dt, \qquad (20)$$

where H is the depth of the mixed layer, h the thickness of the thermocline, ΔU and ΔT are current velocity and temperature differences across the diurnal thermocline, τ_0 momentum flux on the ocean surface, Q_0 the resultant heat influx to the upper $(H + h)$-thick layer of the ocean (taking into account volume absorbtion of solar radiation), t is time (zero time reading corresponds to beginning of the daytime heating period).

If we introduce the averaged value of heat flux, $\langle Q_0 \rangle$, and the averaged value of friction velocity, $\langle U_* \rangle$, by the relations,

$$\langle Q_0 \rangle = t^{-1} \int_0^t Q_0 dt, \ \langle U_* \rangle = (t^{-1} \int_0^t (\tau_0/\rho)dt)^{1/2}, \qquad (21)$$

then, from Eqs. (16), (17), (19), (20) we can obtain:

$$\Delta U/h = \mathrm{Ri}_0^{-1}\langle U_* \rangle/\langle L_* \rangle, \qquad (22)$$

$$\Delta T/h = \mathrm{Ri}_0^{-1}\langle T_* \rangle/\langle L_* \rangle, \qquad (23)$$

$$h/H = (1 + 2\,\mathrm{Ri}_0\langle L_* \rangle\langle U_* \rangle t/H^2)^{1/2} - 1, \qquad (24)$$

where $\langle T_* \rangle = \langle Q_0 \rangle/(c_p\rho\langle U_* \rangle)$, $\langle L_* \rangle = \langle U_* \rangle^3/(\alpha g\langle Q_0 \rangle/c_p\rho)$.

Formulas (22)–(23) interrelate the mean temperature and velocity gradients in the daytime thermocline with the heat and momentum fluxes at the air–sea interface. Equation (24) describes evolution (growth) of the daytime thermocline thickness.

Formulas (22), (23) yield a relation

$$\Delta U/\langle U_* \rangle = \Delta T/\langle T_* \rangle, \qquad (25)$$

that may be used to define velocity difference, ΔU, by applying the temperature difference, ΔT. For the resistance coefficient, $\langle C_u \rangle = (\langle U_* \rangle/\Delta U)^2$, we obtain from the relation (22):

$$\langle C_u \rangle = (\mathrm{Ri}_0\langle L_* \rangle/h)^2. \qquad (26)$$

Instant values of τ_0 and Q_0 should not change much too rapidly so that the time was sufficient for the self-regulating state to set in. According to Barenblatt (1982) the turbulent heat exchange under nonstationary conditions in an environment with highly stable

stratification does not comply with the commonly used equations of turbulence. In such cases, particularly during nighttime deepening of the diurnal thermocline, profiles becomes exponential (Bezverkhnii and Soloviev 1986) in contrast to the linear profiles at the self-regulating state.

Figure 8 examines relation (25) using experimental data obtained in daytime under conditions of large diurnal heating (see Table 1). The mean values of τ_0 and Q_0 have been calculated on the base of ship's meteorological information and relations (21). Taking into account volume absorbtion of solar radiation the heat flux Q_0 in relations (21) has been estimated by the formula $Q_0 \approx Q_T + Q_L + Q_E + 0.65(Q_\Sigma - R_\Sigma)$. According to Fig. 8 the experimental data, despite the scatter, agree with the relation (25). The major cause of the experimental data scatter is apparently linked with calculations of the momentum and heat fluxes at the ocean surface using the bulk parametrization. Besides, during the time interval between the measurements made in the near-surface layer of the ocean the vessel changed its geographic position (see Table 1). An additional error resultant from spatial inhomogeneity of the meteorologic parameter field was therefore introduced in computations of the mean values, $\langle Q_0 \rangle$ and $\langle \tau_0 \rangle$.

c. *Upper velocity limit of the daytime near-surface current*

Hypothesis of self-regulating state of the diurnal thermocline at the daytime allows for estimation of the upper limit of the daytime near-surface current velocity.

Heat content of the surface ocean layer due to daytime solar heating can be written as $\mathcal{J}_0 \approx c_p \rho \Delta T(H + 0.5h)$.

It follows from (17) and from an evident inequality $(H + 0.5h) > 0.5h$ that $\Delta U^2 < 2\ \mathrm{Ri}_0^{-1} \alpha g \mathcal{J}_0/(c_p \rho)$.

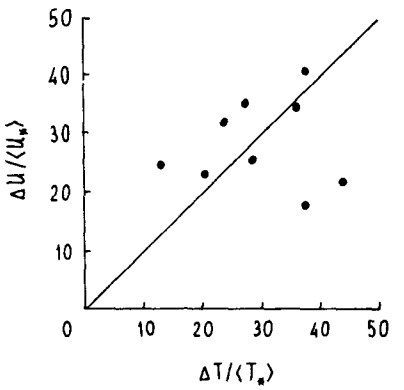

FIG. 8. Experimental testing of relation (25).

Hence, the upper limit of the daytime near-surface current velocity can be expressed as follows:

$$\Delta U_{\max} \approx [2\ \mathrm{Ri}_0^{-1} \alpha g \mathcal{J}/(c_p \rho)]^{1/2}. \quad (27)$$

Heat content variation of the upper layer dictated by the daytime heating is mainly caused by solar absorption. The maximum value of the solar radiation absorbed by the ocean during the daytime is roughly equal to 2×10^7 J m^{-2}. The upper 1-m layer of the ocean absorbs half of this solar radiation, therefore we use an evaluation $\mathcal{J}_0 = 1 \times 10^7$ J m^{-2}. Substituting this value into (27), we obtain $\Delta U_{\max} \approx 29$ cm s^{-1}.

5. Conclusions

We have presented the observations made in the equatorial Atlantic in February–March 1987 during the 35th cruise of the R/V *Akademic Vernadsky,* using a free-rising profiler and drifters which reveal an existance of a near-surface slippery layer of the ocean produced by daytime solar heating. The solar heating warms and stabilizes the surface layer of the ocean. At a low wind speed it suppresses the turbulence and limits the downward penetration of turbulent wind mixing. The upper ocean is slipping over the underlying water practically without friction. The temperature difference in the 5-m ocean layer being about 1°C, the drag coefficient was observed to decrease by a factor of 25 to 30 as compared with the no-stratification case.

Reduction of the drag coefficient contributes to the slipping of the daytime heating layer over the underlying water mass that results in the generation of a daytime near-surface current. The amplitude of the current's diurnal velocity variation becomes larger as the wind speed diminishes (except for the conditions of extremely low wind speed). The velocity of the daytime surface current was observed to reach 19 cm s^{-1}.

The effect of the slipping in the daytime heating layer is explained by the theory of turbulence in stratified environment. A simple one-dimensional integral model simulates the main variations of the diurnal mixed layer, the velocity and temperature differences caused by diurnal heating.

During daytime the diurnal thermocline apparently remains in the self-regulating state characterized by the equilibrium bulk Richardson number, $\mathrm{Ri}_0 = 0.3 \pm 0.1$. The self-regulating regime of the diurnal thermocline results in simple relations (22)–(24) coupling the temperature and velocity differences and the thickness of thermocline. The upper velocity limit of the daytime near-surface current is estimated to be 29 cm s^{-1}.

Acknowledgments. We express our gratitude to Academician G. S. Golitsin for discussion at the initial stage of the work as well as to V. I. Usatchev, V. A. Bezverkhnii, Dr. S. A. Grodsky, and Dr. A. A. Gratchev for their assistance in conducting experiments. Radia-

tion data were provided by Dr. I. N. Plakhina. Model computations were carried out by A. V. Tsvetkov.

REFERENCES

Barenblatt, G. I., 1982: The model of nonstationary turbulent heat and mass exchange in fluid with highly stable stratification. *Fiz. Atmos. Okeana,* **18**(3), 262–268 (in Russian).

——, and G. S. Golitsin, 1973: Local structure of the developed dust storms. Moscow University Press, p. 44 (in Russian).

Bezverkhnii, V. A., and A. V. Soloviev, 1986: Experimental data on the vertical structure of nonstationary near-surface thermocline. *Fiz. Atmos. Okeana,* **22**(1), 71–77 (in Russian).

Bruce, J. G., and E. Firing, 1974: Temperature measurements in the upper 10 m with modified expendable bathythermograph probes. *J. Geophys. Res.,* **79,** 4110–4111.

Cheung, T. K., and R. L. Street, 1988: The turbulent layer in the water at an air-water interface. *J. Fluid Mech.,* **194,** 133–151.

Dillon, T. M., J. C. Richman, G. G. Hansen and M. D. Pearson, 1981: Near-surface turbulence measurements in a lake. *Nature,* **290,** 390–392.

Egorikhin, V. D., V. M. Radikevitch and V. N. Kudryavtsev, 1976: TROPEX-74, v. 2, Leningrad, *Hydrometeoizdat,* 192–195 (in Russian).

Filatov, N. N., S. V. Rjanzin and S. V. Zaycev, 1981: Investigation of turbulence and Langmuir circulation in Lake Ladoga. *J. Great Lakes Res.,* **7,** 1–6.

Houghton, D., 1969: Acapulco'68. *Weather,* **24**(1), 2–18.

Kitaigorodskii, S. A., M. A. Donelan, J. L. Lumley and E. A. Terray, 1983: Wave-turbulent interaction in the upper ocean. Part II: Statistical characteristics of wave and turbulent components of the random velocity field in the marine surface layer. *J. Phys. Oceanogr.,* **13**(11), 1988–1999.

Landau, L. D., and E. M. Lifshits, 1986: Theoretical physics, *Hydrodynamics,* Vol. 6, Moscow, Nauka, 736 p.

Montgomery, R. B., and E. D. Stroup, 1962: Equatorial waters and currents at 150°W in July–August 1952. *John Hopkins Oceanogr. Stud.,* **1,** 68 pp.

Nieuwstadt, F. T. M., 1984: The turbulent structure of the stable, nocturnal boundary layer. *J. Atmos. Sci.,* **41**(14), 2202–2216.

Niiler, P. P., and E. B. Kraus, 1977: One-dimensional models. *Modelling and Prediction of the Upper Layers of the Ocean,* E. B. Kraus, Ed., Pergamon Press, 64–91.

Price, J. F., R. A. Weller and R. Pinkel, 1986: Diurnal cycling: Observations and models of the upper ocean response to diurnal heating, cooling and wind mixing. *J. Geophys. Res.,* **91**(C7), 8411–8427.

Soloviev, A. V., 1982: On vertical structure of the thin surface layer of the ocean at weak winds. *Fiz. Atmos. Okeana,* **18**(76), 751–760 (in Russian).

——, and N. V. Vershinsky, 1982: Vertical structure of the thin surface layer of the ocean under conditions of low wind speed. *Deep-Sea Res.,* **29**(12A), 1437–1449.

——, —— and V. A. Bezverkhnii, 1988: Small-scale turbulence measurements in the thin surface layer of the ocean. *Deep-Sea Res.,* **35**(12A), 1859–1874.

Turner, J. S., 1973: *Buoyancy Effects in Fluids.* Cambridge University Press, 367 pp.

Thorpe, S. A., 1985: Small-scale processes in the upper ocean boundary layer. *Nature,* **318,** 519–522.

Woods, J. D., 1968: An investigation of some physical processes associated with the vertical flow of heat through the upper ocean. *Meteor. Mag.,* **97**(1148), 65–72.

——, and V. Strass, 1986: The response of the upper ocean to solar heating. II. The wind-driven current. *Quart. J. Roy. Meteor. Soc.,* **112**(471), 29–42.